ELSEVIER

Journal of Fluorine Chemistry 110 (2001) 133–138

JOURNAL OF FLUORINE CHEMISTRY

www.elsevier.com/locate/jfluchem

Crystal structure of new hydroxide fluorides with isolated F^- anions: $[H_3N(CH_2)_6NH_3]_2M(F, OH)_6(F,OH)\cdot H_2O$ (M = Al, In)

J. Touret[a], X. Bourdon[b], M. Leblanc[a], R. Retoux[a], J. Renaudin[a], V. Maisonneuve[a,*]

[a]*Laboratoire des Fluorures, UMR 6010, Faculté des Sciences, Université du Maine, Avenue Olivier-Messiaen, 72085 Le Mans Cedex 9, France*

[b]*Laboratoire des Matériaux Minéraux, UPRES-A 7016, Ecole Nationale Supérieure de Chimie de Mulhouse, 3 rue Alfred Werner, 68093 Mulhouse Cedex, France*

Received 27 November 2000; accepted 1 March 2001

Abstract

The synthesis and structural characterization of new hydroxo-fluorometallates $[H_3N(CH_2)_6NH_3]_2M(F,OH)_7\cdot H_2O$ (M = Al, In) are presented. Their preparation is achieved in solvothermal conditions by microwave or classical heating. The isotopic structures, determined by single crystal X-ray diffraction, are triclinic with the space group *P–1*. The structural arrangement can be described from isolated MX_6 (X = F, OH) octahedra connected by diprotonated diaminohexane via a complex network of hydrogen bonds. X^- anions and water molecules are found between the organic chains. A study by ^{19}F NMR of the Al compound confirms a statistical occupancy of fluorine sites by hydroxyl groups and the occurrence of isolated F^- anions.

Keywords: Microwave heating; Hybrid compounds; Fluorides; Nuclear magnetic resonance

1. Introduction

In the last decade, many works have been devoted to the synthesis, the spectroscopic properties, the thermal behavior and structural characterization of fluorometallates with N-containing organic cations ([1] and references therein, [2]). The main interest of these hybrid compounds is their use as precursors for novel fluorinated phases with catalytic applications. In this aim, we focus our research on the synthesis of new hybrid fluorometallates exhibiting a special arrangement, such as cavities, of the metal fluoride polyhedra. Microwave heating proved to be a powerful tool for the exploration of various chemical systems [3–5]. Using this technique, we report here the synthesis and the structural characterization of new hybrid hydroxo-fluorometallates $[H_3N(CH_2)_6NH_3]_2MX_7\cdot H_2O$ (M = Al, In and X = F, OH). In order to confirm the F/OH substitution and the presence of isolated F^- anions, a solid state NMR study was undertaken.

2. Results and discussion

The structure of $[H_3N(CH_2)_6NH_3]_2MX_7\cdot H_2O$ (M = Al, In and X = F, OH) consists of isolated $[MX_6]^{3-}$ anionic octahedra, linked to a 3D network by hydrogen bonds coming from diprotonated DAH and the water molecule (Fig. 1). Along the *b*-axis, the hydrogen atoms of the three crystallographically distinct 1,6-hexanediammonium cations define a square section channel in which isolated F^- anions and water molecules are found. The diprotonated DAH cations and fluoride anions ensure the charge balance. The MX_6 octahedra, which exhibit a very small distortion, rotate alternatively at $\approx\pm 8^\circ$ around the *c*-axis. The mean Al–X and In–X distances, 1.81 and 2.07 Å, respectively, are close to the sum of the ionic radii [6] and are consistent with the observed distances in inorganic fluorometallates. A small elongation of the M2–X5 and M1–X6 bonds can be noted. Diprotonated DAH present a stretched conformation with typical C–C, C–N distances and C–C–C, N–C–C angles; their total length, defined by the distance between the opposite nitrogen atoms (N1–N1, N2–N2, N3–N4), varies from 8.78 to 8.82 Å and from 8.78 to 8.80 Å for the fluoroaluminate and indate, respectively. These values compare very well with those found in ULM 13 (8.72 Å) [7]

* Corresponding author. Tel.: +33-243-833-561; fax: +33-243-833-506.
E-mail address: vincent.maisonneuve@univ-lemans.fr (V. Maisonneuve).

0022-1139/01/$ – see front matter
PII: S0022-1139(01)00420-1

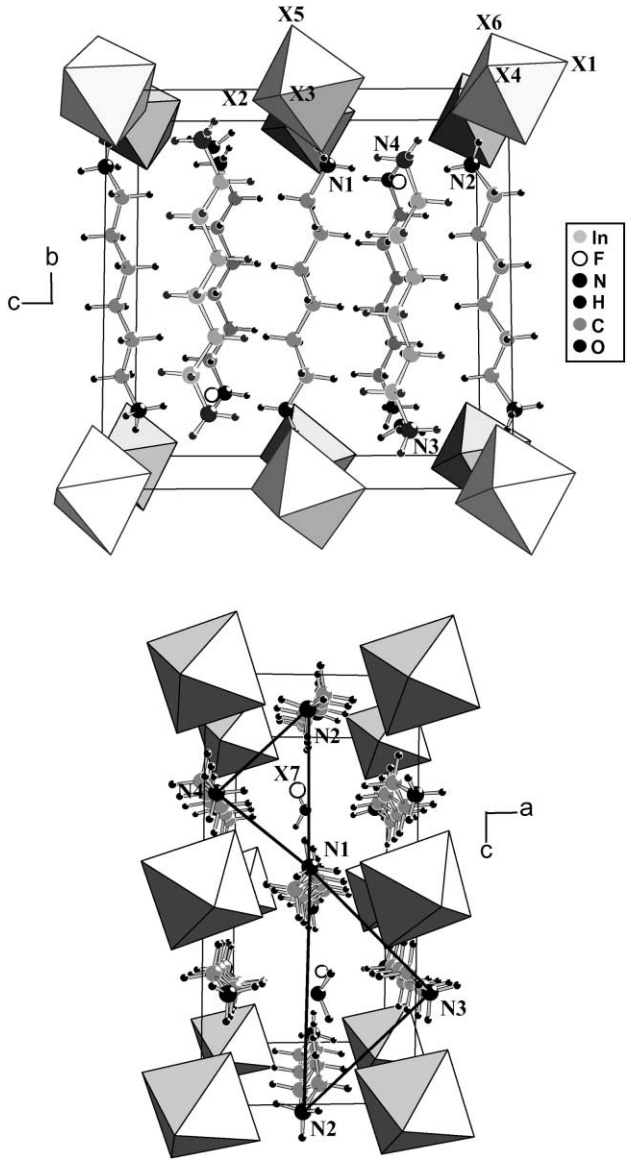

Fig. 1. Perspective views of the $[H_3N(CH_2)_6NH_3]_2MX_7{\cdot}H_2O$ (M = Al, In and X = F, OH) structure.

and $[H_3N(CH_2)_6NH_3]AlF_5$ (8.79 Å) [3]. This structural type shows a great capacity to adapt two very different sizes of cations (ionic radius; $Al^{3+} = 0.535$ Å; $In^{3+} = 0.80$ Å) which implies a variation of the cell volume (>7%). This remark suggests that the synthesis with other trivalent cations of intermediate size such as iron, vanadium, chromium or vanadium can be expected.

The analysis of the hydrogen bond lengths (Table 1) shows a similar behavior for the three different DAH molecules (Fig. 2). Each ammonium cation is strongly linked to isolated octahedra via two hydrogen bonds. The N–X distances vary from 2.70 to 2.89 Å. A third hydrogen bond is found for three independent NH_3 groups (N1, N2, N4) with the isolated X7 anions. This hydrogen bond is strong, the average N–X7 distance, 2.65 Å, is smaller that the other N–X distances. This value compares well to that

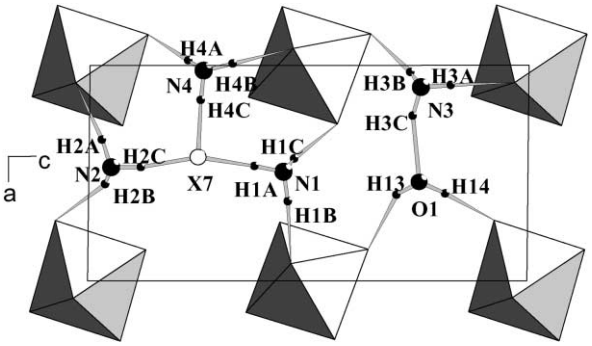

Fig. 2. Hydrogen bond network in $[H_3N(CH_2)_6NH_3]_2MX_7{\cdot}H_2O$ (M = Al, In and X = F, OH).

observed in NH_4F and $N_2H_6F_2$ (from 2.68 to 2.71 Å) [8]. The hydrogen atoms of the water molecule point towards two (F, OH) atoms of two different octahedra (X2, X4). The X7 anion lies inside a small triangle defined by N1, N2 and N4 atoms whereas the water molecule is closer to the MF_6 octahedra than to the N1, N2, N3 atoms (Fig. 1, ac plane). Correlatively, the N1–N2–N3 triangle is larger than the N1–N2–N4 triangle. The presence of this isolated X7 anion is confirmed by the NMR study presented below.

The thermograms of $[H_3N(CH_2)_6NH_3]_2AlX_7{\cdot}H_2O$ exhibit a first weight loss below 150°C attributed to the departure of the water molecule (experimental = 3.9%, theoretical = 4.3%). The thermal evolution of the diffraction pattern shows minor modifications until 150°C. Within 1 day, no weight change under air atmosphere at room temperature is found for the dehydrated phase. Consequently, the departure of the water molecule can be considered as irreversible. Above 150°C, the thermal degradation is complex and occurs in several steps. The XRD pattern of the resulting product presents small peaks with weak broad intensities characteristic of bad crystallinity. Most of the peaks seem compatible with the β-AlF_3 phase.

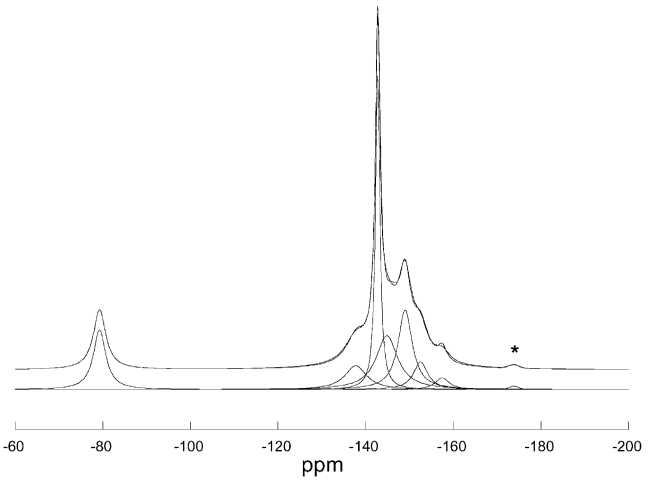

Fig. 3. ^{19}F MAS NMR spectrum (experimental and simulated) of $[H_3N(CH_2)_6NH_3]_2AlX_7{\cdot}H_2O$ (X = F, OH) (∗ spinning side band).

Table 1
Hydrogen bond distances (Å) and angles (°) in $[H_3N(CH_2)_6NH_3]_2MX_7{\cdot}H_2O$ (M = Al, In and X = F, OH)

D–H···A	Aluminum			Indium		
	H···A	D···A	DHA	H···A	D···A	DHA
N4–H4A···X1	1.83	2.699(3)	166.8	1.79	2.668(3)	166.3
N3–H3B···X2	1.91	2.759(3)	159.0	1.91	2.755(4)	156.9
O1–H13···X2	2.02(2)	2.819(3)	150(3)	1.97(2)	2.777(3)	149(4)
N1–H1C···X3	1.92	2.757(3)	155.5	1.91	2.743(3)	154.4
O1–H14···X4	1.885(1)	2.750(3)	167(3)	1.85(1)	2.725(3)	169(4)
N2–H2B···X4	2.11	2.886(3)	145.9	2.08	2.847(3)	143.9
N1–H1B···X5	1.92	2.791(3)	164.2	1.88	2.760(3)	168.7
N4–H4B···X5	1.90	2.783(3)	174.3	1.89	2.776(3)	178.2
N2–H2A···X6	1.87	2.758(3)	176.3	1.89	2.773(3)	172.9
N3–H3A···X6	1.95	2.823(3)	166.9	1.91	2.798(3)	175.5
N1–H1A···X7	1.75	2.640(3)	174.0	1.76	2.645(4)	170.8
N4–H4C···X7	1.78	2.655(3)	166.9	1.77	2.646(4)	168.0
N2–H2C···X7	1.78	2.665(3)	172.0	1.78	2.659(4)	169.3
N3–H3C···O1	2.02	2.892(3)	165.6	2.01	2.854(4)	158.2

The ^{19}F MAS NMR spectrum of $[H_3N(CH_2)_6NH_3]_2$-$AlX_7{\cdot}H_2O$ recorded with a spinning rate of 35 kHz is presented in Fig. 3. It exhibits one main group of resonance peaks between −130 and −160 ppm and one isolated peak at −79.2 ppm. The observed chemical shifts are respectively consistent with fluorine atoms of AlX_6 units [9] and with isolated fluorine F^- observed in NH_4F [10,11]. The best simulation of the experimental spectrum was obtained with seven resonance lines centered at −157.4, −152.5, −149, −145.9, −142.8, −137.9 and −79.2 ppm. One rotation sideband at −173.8 ppm was associated to the isolated resonance at −79.2 ppm. These interpretations are in good agreement with XRD results and thus confirm seven different sites for fluoride anions, including the isolated F^-. The occurrence of this isolated anion is also found in the indium phase (−80 ppm). Similar chemical shifts are encountered for fluoride ion trapped in D4R units in Mu-3 [12] and ULM-5 [13]. In NH_4F and the title compound, fluoride ions adopt a tetrahedral and three-fold hydrogen coordination (Fig. 4), respectively. The area ratio of the seven components is roughly 3/7/21/20/25/10/14 which differs from the 14/14/14/14/14/14/14 expected ratio. These results and the fluorine chemical analysis (4.3 F per unit) suggest a strong F/OH substitution. Similar situations were encountered in many closed systems ([14] and references therein). The F/OH substitution differs clearly for each site and the estimated F/OH ratio is 12/88, 28/72, 84/16, 80/20, 100/0, 40/60, 56/44 consistent with the presence of 4.0 F per formula unit. The ^1H MAS NMR spectra do not allow to distinguish the different surroundings types of hydrogen atoms (CH_2, NH_3, H_2O and OH). ^1H CRAMPS experiments are currently underway to confirm the substitution rates on each site. An attribution of the six fluoride sites of the AlX_6 octahedra to the resonance components in the range −130, −160 ppm will be investigated further by ^{19}F CRAMPS and $^{27}Al-^{19}F$ HETCOR experiments.

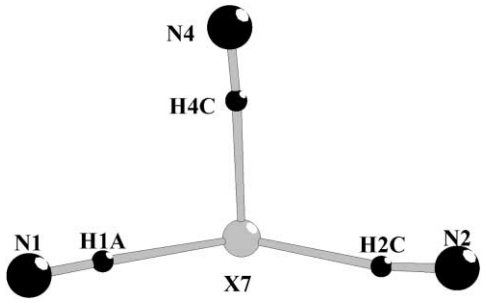

Fig. 4. Coordination of isolated X anion in $[H_3N(CH_2)_6NH_3]_2MX_7{\cdot}H_2O$ (M = Al, In and X = F, OH).

3. Experimental

3.1. Experimental part

The title compounds were prepared by microwave synthesis under autogeneous pressure from a mixture of M_2O_3 (M = Al, In), 6 M HF, 1,6-diaminohexane (DAH) and ethanol in the molar ratio 0.5:6:2:170. After a quick stirring, each starting mixture was introduced into Teflon autoclaves, and then placed on the carrousel of a CEM microwave oven (MDS 2100). In this synthesis, the order of introduction of the reagents in the autoclave is decisive: M_2O_3–ethanol–HF–DAH. The modification of this order leads to a product showing a X-ray diagram with a first intense peak at the same angular position as the initial diagram but with different positions of the following peaks. The synthesis, regulated in pressure (P_{max} = 23 bars), was performed at $T \approx 190°C$ during 1 h and followed by cooling to room temperature. The resulting crystalline products were washed with ethanol and acetone and dried at 40°C. Owing to the relative solubility of the title compounds in polar solvents (water, ethanol, acetone), it is necessary to process this last step quickly. Each product contains numerous translucent platelets, suitable for a structural determination (Fig. 5). By

Fig. 5. SEM image of $[H_3N(CH_2)_6NH_3]_2AlX_7{\cdot}H_2O$ (X = F, OH) crystals.

comparison of the simulated and experimental X-ray powder patterns, which show a first intense peak followed by weak reflections, traces of unknown impurities were detected. Attempts in classical hydrothermal autoclaves led to larger crystals of the same compounds. However, the obtained powders contain more impurities. Thermal gravimetric analyses of the aluminum phase were performed on a TGA92 Setaram apparatus under argon gas flow (heating rate 10°C/min between 300 and 900 K). X-ray thermodiffractometry of the aluminum phase was carried out under air on a Siemens D5000 diffractometer (Cu Kα radiation) equipped with a linear Elphyse detector. The fluorine content of the Al phase was determined by the potentiometric method with a fluorine-specific electrode. The experimental result was found smaller (≈20%) than the theoretical value (≈32%). This chemical analysis indicates clearly the occurrence of a F/OH substitution. The number of fluorine atoms per formula is close to 4.3. The NMR experiments were performed with Bruker spectrometers MSL 300 (CP MAS ^{13}C, ^{1}H MAS NMR) or DSX 400 (^{1}H and ^{19}F MAS NMR). The ^{13}C and ^{1}H NMR spectra are not discussed here and will be presented elsewhere. The ^{19}F MAS NMR spectra were recorded with a 2.5 mm Bruker MAS probe allowing high spinning frequencies. A spin-echo pulse sequence ($\pi/2$–τ–π) was used with a $\pi/2$ pulse length of 1.8 μs, $\tau = 28.6$ μs and a recycle delay of 5 s. The spectra were obtained by using different speeds in the range 8–35 kHz in order to ascertain the isotropic resonance positions. The chemical shifts were referenced to $CFCl_3$. Data analysis was carried out by using the Bruker commercial programs WINNMR and WINFIT [15].

3.2. Structural determination

A single crystal of each compound was isolated under an optical microscope. The unit cell parameters were obtained from a random reflection search and X-ray diffraction data were collected on a Siemens AED2 four-circle diffractometer. The intensities of each set of reflections were corrected for Lorentz and polarization effects but no absorption correction was applied. The scattering factors and the anomalous dispersion corrections for all atoms were taken from ''International Tables for X-ray Crystallography'' [16]. Table 2 gathers the crystallographic data and information on

Table 2
Crystallographic data for $[H_3N(CH_2)_6NH_3]_2MX_7{\cdot}H_2O$ (M = Al, In and X = F, OH)

M	Al	In
Crystal system, space group	Triclinic, *P–1*	
Cell dimensions		
a (Å)	6.300(2)	6.4714(3)
b (Å)	12.690(2)	12.9203(9)
c (Å)	12.742(1)	13.0843(6)
α (°)	90.97(1)	90.160(6)
β (°)	90.52(1)	90.683(4)
γ (°)	94.35(2)	94.138(5)
V (Å^3), Z	1015.7(3), 2	1091.06(2), 2
Temperature (K)	293	
Absorption correction, coefficient (mm^{-1})	Not applied, 0.17	Not applied, 1.13
Crystal shape, color, size (mm)	Lamella, colorless, 0.15 × 0.11 × 0.06	Lamella, colorless, 0.38 × 0.23 × 0.08
Molecular weight (g/mol)	414.43	502.27
$\rho_{calc.}$ (g/cm^3)	1.355	1.529
Radiation, λ (Å)	Mo Kα, 0.71069	
Diffractometer	AED2–STOE	
2θ range for data collection (°)	2–50	2–55
Reflection and parameter numbers	3582, 241	5013, 241
Goodness-of-fit on F^2	1.058	1.060
$(hkl)_{min}$, $(hkl)_{max}$	−7 −15 −15, 7 15 15	−8 −16 0, 8 16 16
R_1 (I > 2σ(I)), wR_2 (all data)	0.045, 0.098	0.031, 0.080
Final Fourier residuals (min/max) (e$^-$/Å^3)	−0.21/0.25	−0.68/0.84
Extinction coefficient	1.0(1) × 10^{-5}	6(4) × 10^{-7}

data collections. Metal and (F, OH) positions were disclosed by direct methods of the program SHELXS-86 [17]. The structure refinements were performed using the SHELXL-97 program [18]. Nitrogen or carbon atoms were located by difference Fourier maps. The location of the hydrogen atoms of the organic chains was performed by applying geometrical constraints (HFIX option in SHELXL-97 program). The positions of the hydrogen atoms of the water molecules were only constrained in distance with a DFIX option. The final refinements with anisotropic atomic displacement parameters (ADP) for all non-hydrogen atoms converged to a reliability factor $R_1 = 0.045$ and $R_1 = 0.031$ for the aluminum and indium phases, respectively. The small size of the crystal of $[H_3N(CH_2)_6NH_3]_2AlX_7{\cdot}H_2O$ led to higher reliabilities compared to those of $[H_3N(CH_2)_6NH_3]_2InX_7{\cdot}H_2O$. The substitution of fluorine atoms by oxygen atoms and the substitution of the oxygen atom of the water molecule by a fluorine atom led systematically to an increase of the reliability factors. Owing to the large equivalent isotropic ADP, no discussion of the influence of F/OH substitution on M–X bond lengths was undertaken. The refined atomic coordinates with equivalent isotropic ADP and selected distances are listed in Tables 3 and 4, respectively. Structure projections were drawn with the DIAMOND program [19]. Crystallographic data (excluding structure factors) for the structures in this paper have been deposited with the

Table 3
Positional and isotropic equivalent atomic displacement parameters for $[H_3N(CH_2)_6NH_3]_2MX_7{\cdot}H_2O$ (M = Al, In and X = F, OH)[a]

M	Aluminum				Indium			
Atom	X	Y	Z	B_{eq} (Å^2)*	X	Y	Z	B_{eq} (Å^2)*
M1	0	0	0	1.69(2)	0	0	0	1.812(7)
M2	0	0	1/2	1.78(2)	0	0	1/2	1.863(7)
X1	0.1496(2)	0.0411(1)	−0.1134(1)	2.47(3)	0.1439(3)	0.0510(2)	−0.1313(1)	2.95(3)
X2	0.1560(2)	0.0154(1)	−0.6184(1)	2.63(3)	0.1461(3)	0.0149(2)	−0.6390(2)	3.17(4)
X3	0.2334(2)	−0.0352(1)	−0.4316(1)	2.53(3)	0.2725(3)	−0.0401(2)	−0.4356(2)	2.90(3)
X4	0.2381(2)	0.0227(1)	0.0801(1)	2.50(3)	0.2798(3)	−0.0276(2)	0.0755(2)	3.05(4)
X5	0.0674(2)	0.1390(1)	−0.4637(1)	2.42(3)	0.0790(3)	0.1560(1)	−0.4624(1)	2.66(3)
X6	0.0645(2)	−0.1360(1)	−0.0260(1)	2.38(3)	0.0801(3)	−0.1506(1)	−0.0325(1)	2.64(3)
X7	−0.4343(2)	0.1969(1)	−0.2473(1)	3.39(3)	−0.4249(3)	0.2080(2)	0.2481(2)	3.60(4)
N1	0.4888(4)	−0.1572(2)	−0.5498(2)	2.49(4)	0.4949(4)	−0.1645(2)	−0.5563(2)	2.65(5)
H1A	0.4681	−0.1660	−0.6187	3.7(1)	0.4679	−0.1721	−0.6228	4.1(2)
H1B	0.6267	−0.1419	−0.5365	3.7(1)	0.6310	−0.1535	−0.5462	4.1(2)
H1C	0.4153	−0.1045	−0.5266	3.7(1)	0.4316	−0.1106	−0.5325	4.1(2)
C1	0.4164(4)	−0.2556(2)	−0.4960(2)	2.58(5)	0.4187(6)	−0.2596(2)	−0.5019(3)	2.98(6)
C2	0.5319(5)	−0.3497(2)	−0.5334(2)	2.87(5)	0.5291(6)	−0.3533(3)	−0.5366(3)	3.27(7)
C3	0.4460(5)	−0.4514(5)	−0.4824(2)	3.18(6)	0.4457(6)	−0.4520(3)	−0.4834(3)	3.72(7)
N2	0.4748(3)	−0.1571(2)	0.0435(2)	2.41(4)	0.4729(4)	−0.1647(2)	0.0509(2)	2.68(5)
H2A	0.3434	−0.1472	0.0215	3.7(1)	0.3438	−0.1580	0.0292	4.1(2)
H2B	0.5603	−0.0999	0.0301	3.7(1)	0.5509	−0.1069	0.0376	4.1(2)
H2C	0.4740	−0.1683	0.1122	3.7(1)	0.4731	−0.1761	0.1180	4.1(2)
C4	0.5524(4)	−0.2498(2)	−0.0122(2)	2.34(5)	0.5574(5)	−0.2531(2)	−0.0020(3)	2.70(6)
C5	0.4501(4)	−0.3522(2)	0.0285(2)	2.66(5)	0.4548(6)	−0.3561(2)	0.0328(3)	2.96(6)
C6	0.5458(5)	−0.4473(2)	−0.0217(2)	2.76(5)	0.5468(6)	−0.4480(2)	−0.0190(3)	3.22(6)
N3	0.0701(4)	−0.1345(2)	−0.2474(2)	2.85(5)	0.1008(5)	−0.1357(2)	−0.2455(2)	3.10(5)
H3A	0.0487	−0.1306	−0.1786	3.7(1)	0.0925	−0.1369	−0.1776	4.1(2)
H3B	0.0060	−0.0834	−0.2790	3.7(1)	0.0320	−0.0837	−0.2698	4.1(2)
H3C	0.2091	−0.1272	−0.2600	3.7(1)	0.2331	−0.1268	−0.2634	4.1(2)
C7	0.0190(5)	−0.2385(2)	−0.2886(2)	2.74(5)	0.0089(6)	−0.2350(3)	−0.2880(3)	3.19(6)
C8	0.0784(5)	−0.3286(2)	−0.2359(2)	3.17(6)	0.1000(6)	−0.3268(3)	−0.2398(3)	3.46(7)
C9	0.0179(5)	−0.4353(2)	−0.2781(2)	3.11(6)	−0.0018(7)	−0.4291(3)	−0.2812(3)	3.70(7)
C10	0.0758(4)	0.4708(2)	−0.2281(2)	3.15(6)	0.0839(7)	0.4767(3)	−0.2321(3)	3.80(7)
C11	0.0164(4)	0.3647(2)	−0.2712(2)	2.61(5)	−0.0096(6)	0.3745(3)	−0.2750(3)	3.04(6)
C12	0.0742(4)	0.2742(2)	−0.2143(2)	2.55(5)	0.0728(6)	0.2828(2)	−0.2201(3)	2.90(6)
N4	0.0208(4)	0.1699(2)	−0.2523(2)	2.43(4)	−0.0235(4)	0.1830(2)	−0.2592(2)	2.66(5)
H4A	0.0261	0.1193	−0.2126	3.7(1)	0.0237	0.1311	−0.2232	4.1(2)
H4B	0.0165	0.1594	−0.3186	3.7(1)	0.0082	0.1756	−0.3247	4.1(2)
H4C	−0.1619	0.1685	−0.2484	3.7(1)	−0.1605	0.1821	−0.2531	4.1(2)
O	0.4700(4)	0.1085(2)	−0.7512(2)	3.40(4)	0.4571(4)	0.1170(2)	−0.7529(2)	3.85(5)
H13	0.414(4)	0.074(2)	−0.697(2)	3.7(1)	0.398(6)	0.081(3)	−0.702(2)	4.1(2)
H14	0.415(4)	0.079(2)	−0.809(1)	3.7(1)	0.404(6)	0.096(3)	−0.813(2)	4.1(2)

[a] Hydrogen atomic positions of CH_2 groups can be obtained from the authors.

Table 4
Selected distances (Å) and angles (°) in $[H_3N(CH_2)_6NH_3]_2MX_7{\cdot}H_2O$ (M = Al, In and X = F, OH)

	Aluminum	Indium		Aluminum	Indium
M1–X1 (×2)	1.795(1)	2.052(2)	X1–M1–X4 (×2)	90.33(7)	88.10(8)
M1–X4 (×2)	1.809(1)	2.060(2)	X1–M1–X4 (×2)	89.67(7)	91.90(8)
M1–X6 (×2)	1.828(2)	2.093(2)	X1–M1–X6 (×2)	89.37(7)	90.58(7)
$M1–X_{average}$	1.811	2.068	X1–M1–X6 (×2)	90.63(7)	89.42(7)
			X4–M1–X6 (×2)	90.12(7)	90.97(8)
			X4–M1–X6 (×2)	89.88(7)	89.03(8)
M2–X3 (×2)	1.793(2)	2.046(2)	X3–M2–X5 (×2)	89.54(7)	89.81(7)
M2–X2 (×2)	1.813(1)	2.062(2)	X3–M2–X5 (×2)	90.46(7)	90.19(7)
M2–X5 (×2)	1.833(1)	2.099(2)	X3–M2–X2 (×2)	90.93(7)	90.99(8)
$M2–X_{average}$	1.813	2.069	X3–M2–X2 (×2)	89.87(7)	89.01(8)
			X2–M2–X5 (×2)	90.50(7)	92.01(8)
			X2–M2–X5 (×2)	89.50(7)	87.99(8)
N1–C1	1.478(3)	1.478(4)	N1–C1–C2	112.5(2)	111.5(3)
C1–C2	1.517(4)	1.521(5)	C1–C2–C3	111.8(2)	111.5(3)
C2–C3	1.521(4)	1.522(5)	C2–C3–C3	114.2(3)	112.9(4)
C3–C3	1.516(5)	1.534(7)			
N2–C4	1.481(3)	1.476(4)	N2–C4–C5	111.7(2)	111.7(3)
C4–C5	1.507(4)	1.517(4)	C4–C5–C6	111.4(2)	111.9(3)
C5–C6	1.524(4)	1.527(5)	C5–C6–C6	113.0(3)	112.6(4)
C6–C6	1.530(5)	1.522(7)			
N3–C7	1.480(3)	1.479(4)	N3–C7–C8	112.6(2)	112.1(3)
C7–C8	1.503(4)	1.500(5)	C7–C8–C9	111.4(2)	111.7(3)
C8–C9	1.528(4)	1.528(5)	C8–C9–C10	113.6(2)	112.8(3)
C9–C10	1.517(4)	1.515(5)	C9–C10–C11	113.8(2)	113.6(3)
C10–C11	1.518(4)	1.516(5)	C10–C11–C12	111.4(2)	111.7(3)
C11–C12	1.513(4)	1.512(5)	C11–C12–N4	112.2(2)	111.9(3)
C12–N4	1.482(4)	1.479(5)			
N–H	0.97	C–H	0.89	O–H	0.89(1)

Cambridge Crystallographic Data Center as supplementary publication nos. CCDC 160619 and 160620. Copies of the data can be obtained, free of charge, on application to CCDC, 12 Union Road, Cambridge CB2 1EZ, UK (fax: +44-1223-336033 or deposit@ccdc.cam.ac.uk).

Acknowledgements

The authors are indebted to Dr. Luc Delmotte for helpful discussions on the NMR part.

References

[1] U. Bentrup, M. Feist, E. Kemnitz, Prog. Solid St. Chem. 27 (1999) 75–129.
[2] S.M. Walker, P.S. Halasyamani, S. Allen, D. O'Hare, J. Am. Chem. Soc. 121 (1999) 10513–10521.
[3] S. Phan Thanh, F. Gaslain, M. Leblanc, V. Maisonneuve, J. Fluorine Chem. 101 (2000) 161–163.
[4] S. Phan Thanh, J. Renaudin, V. Maisonneuve, Solid State Sci. 2 (2000) 143–148.
[5] G. Corbel, G. Courbion, F. Le Berre, M. Leblanc, J.M. Le Meins, V. Maisonneuve, N. Mercier, J. Fluorine Chem. 107 (2001) 193–198.
[6] R.D. Shannon, Acta Crystallogr. A 32 (1976) 751–767.
[7] J. Renaudin, G. Férey, J. Solid State Chem. 120 (1995) 197–203.
[8] A.F. Wells, Structural Inorganic Chemistry, 5th Edition, Clarendon Press, Oxford, 1986.
[9] E.A. Goreshnik, F. Taulelle, M. Leblanc, V. Maisonneuve, Solid State Sciences, 2000, submitted for publication.
[10] J.M. Emsley, J. Feeney, L.H. Sutcliffe, High Resolution Nuclear Magnetic Resonance Spectroscopy, Vol. 2, Pergamon Press, Oxford, 1966, p. 881.
[11] L. Delmotte, Personal data base collection, unpublished results.
[12] P. Reinert, J. Patarin, T. Loiseau, G. Férey, H. Kessler, Microporous Mesoporous Mater. 22 (1998) 43–55.
[13] T. Loiseau, D. Riou, F. Taulelle, G. Férey, Zeolites and Related Microporous Mater. 84 (1994) 395–402.
[14] T. Loiseau, F. Taulelle, G. Férey, Microporous Mater. 5 (1996) 365–379.
[15] D. Massiot, Winfit version 990420, Centre de Recherches sur les Matériaux à haute température, Orléans, http://crmht.cnrs-orleans.fr/Pole1/ThemeDM/dmfit, 1999.
[16] International Tables for X-ray Crystallography, Vol. IV, Kynoch Press, Birmingham, UK, 1974.
[17] G.M. Sheldrick, SHELXS-86, in: G.M. Sheldrick, C. Krüger, R. Goddard (Eds.), Crystallographic Computing 3, Oxford University Press, Oxford, 1985, pp. 175–189.
[18] G.M. Sheldrick, SHELXL-97, A Program for Crystal Structure Determination, Göttingen University, Germany, 1997.
[19] G. Bergerhoff, DIAMOND Visual Crystal Structure Information System, Gerhard-Domagk-Str. 1, 53121 Bonn, Germany, 1996.